

# Quantitative Geomorphology Related to Active Tectonics in The Cilayu Watershed, West Java Province, Indonesia

Mirza Muhajir<sup>1</sup>; Emi Sukiyah<sup>2</sup>; Reza Mohamad Ganjar Gani<sup>3</sup>

Geological Engineering Program, Faculty of Geological Engineering, Universitas Padjadjaran, Jl. Raya Bandung-Sumedang KM.21, Sumedang, 45363, Indonesia<sup>1</sup>

Geomorphology & Remote sensing Laboratory, Faculty of Geological Engineering, Universitas Padjadjaran, Jl. Raya Bandung-Sumedang KM.21, Sumedang, 45363, Indonesia<sup>2</sup>

Stratigraphy Laboratory, Faculty of Geological Engineering, Universitas Padjadjaran, Jl. Raya Bandung-Sumedang KM.21, Sumedang, 45363, Indonesia<sup>3</sup>

[mirza16001@mail.unpad.ac.id](mailto:mirza16001@mail.unpad.ac.id)<sup>1</sup>; [emi.sukiyah@unpad.ac.id](mailto:emi.sukiyah@unpad.ac.id)<sup>2</sup>; [reza.mohammad@unpad.ac.id](mailto:reza.mohammad@unpad.ac.id)<sup>3</sup>

DOI < 10.26821/IJSHRE.8.7.2020.8706 >

## ABSTRACT

The Cilayu watershed is selected to analyze and predict relative tectonic activity based on geomorphic indices. This area is prone to earthquakes originating from subduction zones at sea and active faults on land. To assess tectonic activity in the area, we analyzed five geomorphic indices: the mountain front sinuosity index (Smf), valley floor width-to-height ratio (Vf), drainage basin asymmetry factor (Af), drainage basin shape (Bs), and hypsometric integral (Hi). Then based on the index of active tectonics (IAT) values calculated by the average of five geomorphic indices, relative tectonic activity levels revealed. The research area proved to be an active tectonic area, confirmed by values of AF, Bs, Vf, Smf, and Hi. Value of AF 24.83 - 67.77, Bs 0.97 - 3.81, Vf 0.17 - 7.03, Smf 1.16 - 2.54, and Hi 0.31 - 0.61 showing that some area in Cilayu watershed has been affected by active tectonics. The drainage patterns that can be recognized are trellis, parallel, and rectangular. On the other hand, these drainage patterns reflect the control of geological structures. The study area was divided into three parts: Class 1 (very high tectonic activity, 1.78% in area); Class 2 (high, 7.03%); Class 3 (moderate, 30.68%), and Class 4

(low, 9.69%). The results are consistent with field observations on landforms and geology.

**Keywords:** Morphotectonic; Geomorphic Indices; Cilayu watershed; IAT.

## 1. INTRODUCTION

In areas affected by moderate tectonic deformation rates, geomorphology and geological data provide some of the best information to support and characterize active tectonics [1],[2], [3].

One exciting area to study to characterize the active tectonic effect is the Cilayu watershed, West Java. This area is one of the earthquake-prone areas originating from subduction zones at sea and active faults on land. Therefore it is crucial to analyze the activity level of the Cilayu watershed from the geomorphological study.

To characterize the geomorphic features of a landscape, quantitative geomorphic analyses (morphotectonics) conducted using geomorphic indices, which help to assess the relative level of tectonic activity in an area [4], [5], [6], [7], [8].

Morphotectonics can express a roman topographic view that can use as an indicator of the style, strength, and average tectonic movement. In other words, the tectonic activity of a location known as

supported by qualitative spatial data and geomorphology. With the method used in this study, it is expected that the results would be a general picture of tectonic activity in the research area with a fast and efficient process.

The Cilayu upstream to downstream distinguished in several morphographic units such as mountains, hills, valleys, and plains [9]. The different slope affects the drainage pattern in the Cilayu watershed. The drainage patterns that can be recognized are trellis, parallel, and rectangular. All of the drainage patterns reflect the control of geological structures.

According to [10] and [11], the study area composed of 7 rocks formations (Fig.1). In general, these formations consist of tertiary sedimentary rocks (Tmk, Tmpb), which form tuff sandstone, pumice tuff, claystone, conglomerate, lignite, and breccia. Volcanic rocks that form well-cemented breccia (Tomj), lavas, tuff, and tuff breccia (QTV, Tpv), alternation of lavas breccia and tuff, pyroxene-andesitic and hornblende-andesitic composition (Qwb). Intrusive rocks which form pyroxene andesitic (pa) and quartz diorite (Tmi (d)).

**Fig 1: Regional geology of the study area is showing the distribution of lithology from different rocks formations in Cilayu Watershed (Modified from [10] and [11]).**

## 2. MATERIAL AND METHOD

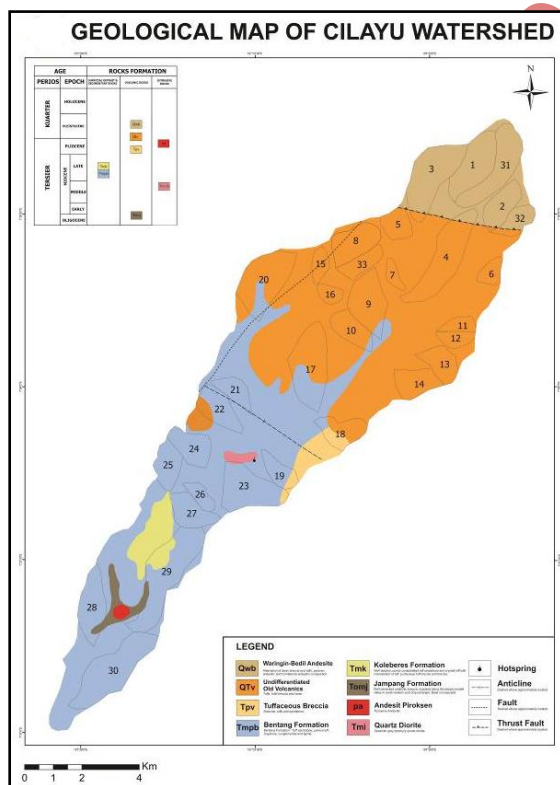
This study aims to identify the index of active tectonics (*IAT*) based on quantitative geomorphology analysis. Parameters subjects in this research of the Cilayu watershed, which consists of drainage basin asymmetry (*AF*), hypsometric-integral (*Hi*), valley floor width–valley height ratio (*Vf*), drainage basin shape (*Bs*), and mountain-front-sinuosity (*Smf*).

The methodology relies on the identification and interpretation of topographic map (Topographic map of Indonesia), Geological Map [10,11], Digital Elevation Model (DEM) of Cilayu watershed. The data from DEMNAS in the laboratory using computer program supporting Geographical Information System (GIS) software and field observation to Cilayu watershed.

### 2.1 Geomorphic Indices

Geomorphic indices useful for studying active tectonics include drainage basin asymmetry (*AF*), hypsometric-integral (*Hi*), valley floor width–valley height ratio (*Vf*), drainage basin shape (*Bs*), and mountain-front-sinuosity index (*Smf*) [7].

The geomorphic indices of active tectonics calculated by using a topographic map and DEM. On the other hand, the area divided into 33 sub-watershed, and for each one, the above indices calculated. All of the indices were combined to obtain the index of active tectonics (*IAT*) [13]. Therefore, sub-basins can compare together.



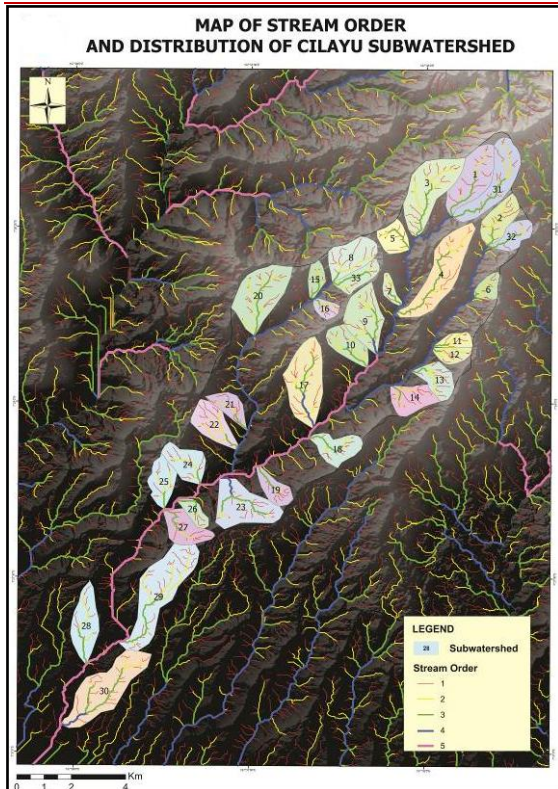


**Fig 2: Stream order map and distribution of Cilayu sub-watershed.**

### 2.1.1 Asymmetry Factor (*AF*)

The asymmetric factor (*AF*) can be used to evaluate tectonic tilting [7], [12]. *AF* is defined as:

$$AF = 100 (A_r / A_t) \quad (1)$$

$A_r$  is the area of a part of the watershed on the right of the master stream (looking downstream), and  $A_t$  is the total area of the watershed. Both  $A_r$  and  $A_t$  measured in GIS Software. If  $AF > 50$ , it indicates that the tilting direction of the basin is to the left (from downstream point of view). However, if  $AF < 50$ , it indicates that the tilting direction is to the right side of the basin [7]. *AF* values were grouped into three classes: 1 ( $AF \geq 65$  or  $AF < 35$ ); 2 ( $35 \leq AF < 43$  or  $57 \leq AF < 65$ ), and 3 ( $43 \leq AF < 57$ ) [13]. (Table I).

Then, to show the extent to which the asymmetry develops in a watershed, the *AF* value is expressed as an absolute value minus 50, added with arrows indicating the direction of the asymmetry [14]. Then *AF* absolute values were grouped into four classes:  $AF < 5$  (symmetric basins),  $AF = 5-10$  (gently asymmetric basins),  $AF = 10-15$  (moderately asymmetric basins), and  $AF > 15$  (strongly asymmetric basins) [14].

### 2.1.2 Basin Shape Index (*Bs*)

The Basin shape index (*Bs*) is a comparison between basin length (*Bl*) or watershed length measured from the highest point with basin width (*Bw*) axis or watershed width measured from the widest [15]. Relatively young drainage basins in active tectonic areas tend to be elongated in shape, normal to the topographic slope of a mountain [17], [18]. *Bs* value in more active tectonics will be elongated and will become circular after the tectonic process has slowed or stopped. The value of *Bs* calculated using this question:

$$Bs = Bl / Bw(2)$$

*Bs* values computed using a topographic map, and DEM then grouped into three classes; class 1 ( $Bs \geq 4$ ), class 2 ( $3 \leq Bs < 4$ ), and class 3 ( $Bs \leq 3$ ) [13]. (Table 1).

### 2.1.3 Valley floor width-valley height ratio (*Vf*)

The valley width and height ratio (*Vf*) is one of the calculations that can characterize the existence of an active fault. Calculations that can use to determine the occurrence of uplift that occurs can use the ratio between the width of the valley floor with the height of the valley, better known as *Vf* [16], formulated as follows:

$$Vf = 2Vfw / [(Eld - Esc) + (Erd - Esc)] \quad (3)$$

$Vfw$  is the width of the valley floor. *Eld*, *Erd*, and *Esc* are the river elevations – left, right, and center and divided valleys lead to downstream and the stream channel, respectively.  $Vfw$  was calculated for the main valleys in the study area using crosssections drawn from the DEM and the digitized 1:25,000 topographic map. Then  $Vfw$  was classified into three classes: 1 ( $Vf \leq 0.5$ ); 2 ( $0.5 \leq Vf < 1.0$ ) and 3 ( $Vf \geq 1$ ) [13] (Table 1).

### 2.1.4 Mountain-front sinuosity index (*Smf*)

[16] and [18] define the mountain-front-sinuosity index (*Smf*) as a comparison between the planimetric length of a mountain front along the mountain-piedmont junction (*Lmf*) and the straight-line length of the front (*Ls*), expressed equation as follows:

$$Smf = Lmf / Ls \quad (4)$$

The values of *Smf* calculated for 17 mountain fronts using *Lmf* and *Ls* values measured from DEM and a topographic map and divided into three

classes: 1 ( $Smf < 1.1$ ), 2 ( $1.1 \leq Smf < 1.5$ ), and 3 ( $Smf \geq 1.5$ ) [13] (Table 1).

### 2.1.5 Hypsometric Integral ( $H_i$ )

The hypsometric integral ( $H_i$ ) describes the relative distribution of elevation in a given area of a landscape, particularly a drainage basin [19]. Hypsometric Integral is an area located on the curve of the hypsometry. Hypsometric Integral is giving the symbol  $H_i$  calculated in the watershed using Equation 5.

$$H_i = \frac{\text{avrg.elev} - \text{min.elv}}{\text{max.elv} - \text{min.elv}} \quad (5)$$

Using Eq. (5), we computed  $H_i$  for each sub-watershed. Then  $H_i$  values were grouped into three classes to the convexity or concavity of the hypsometric curve: Class 1 with convex hypsometric curves ( $H_i \geq 0.5$ ); Class 3 with concave hypsometric curves ( $H_i < 0.4$ ); and Class 2 with concave-convex hypsometric curves ( $0.4 \leq H_i < 0.5$ ) [13] (Table 1).

### 2.1.6 Index of Active Tectonics ( $IAT$ )

This index represents a summary and average of calculated geomorphic indices used in this study. The value of  $IAT$  calculated using this question:

$$IAT = S / n \quad (6)$$

Where  $S$  represents the sum of geomorphic indices,  $n$  represents the number of selected indices [13]. The values of this index were grouped into four classes to define the degree of active tectonics; 1—very high ( $1.0 \leq IAT < 1.5$ ); 2—high ( $1.5 \leq IAT < 2.0$ ); 3—moderate ( $2.0 \leq IAT < 2.5$ ); and 4—low ( $2.5 \leq IAT$ ) [13]. The ranges of geomorphic indices related to the Index of Active Tectonics ( $IAT$ ) shown in Table 1.

**Table 1. The Range of Geomorphic Indices Refers To [13]**

Aspect	Relative Tectonic Activity		
	Class 1 (High)	Class 2 (Moderate)	Class 3 (Low)
$AF$	$(Af \geq 65)$ or $(Af < 35)$	$(35 \leq Af < 43)$ or $(57 \leq Af < 65)$	$(43 \leq Af < 57)$
$B_s$	$(B_s \geq 4)$	$(3 \leq B_s < 4)$	$(B_s \leq 3)$
$V_f$	$(V_f \leq 0.5)$	$(0.5 \leq V_f < 1.0)$	$(V_f \geq 1)$
$Smf$	$(Smf < 1.1)$	$(1.1 \leq Smf < 1.5)$	$(V_f \geq 1)$
$H_i$	$(H_i \geq 0.5)$	$(0.4 \leq H_i < 0.5)$	$(H_i < 0.4)$

## 2.2 Field Observation

The field observation aims to provide valid data related to geological structures in the study area compared with geomorphic indices calculation results. We recognize the fault scarp, ridge/valley lineament, and rockslide phenomenon as the presence of geological structures in the study area. Moreover, we conducted the measurements of joints to define the trend of the tectonic stress that occurs in the study area. The rosette diagrams inform about the fracture trend while the stereonet inform about the trend of the stress which symbolizes with  $\sigma$  (Sigma).

## 3. RESULT AND DISCUSSION

### 3.1 The Asymmetry Factor ( $AF$ )

$AF$  is close to 50 if there is no or little tilting perpendicular to the direction of the master stream.  $AF$  is significantly higher or smaller than 50 under the effects of active tectonics or substantial lithologic control [15].

The results of the calculation of  $AF$  values in the study area showed  $AF$  values varied from 24.83 (Sub-watershed 14) to 67.77 (Sub-watershed 9). There are 10 sub-watersheds with  $AF$  values which are classified into tectonic class 1 (High): 3(67.73), 6(28.79), 9(67.77), 10(32.12), 14(24.83), 15(65.63), 18(26.85), 20(65.06), 21(28.87), and 33(28.87). Ten sub-watersheds have  $AF$  values that classified into tectonic classes 2 (Moderate), and the other 13 have  $AF$  values that classified into tectonic classes 3 (Low) (Fig.3) (Table 2).

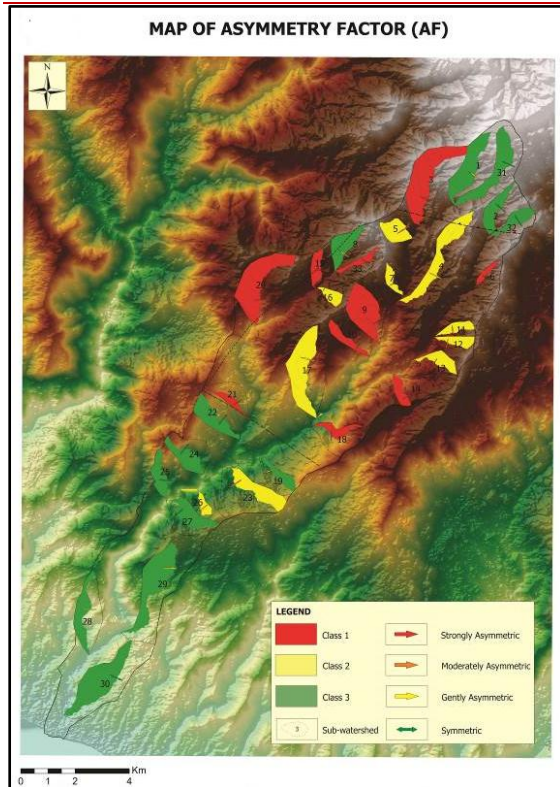


Fig3: Distribution of the Asymmetry Factor (AF) class in Cilayu Watershed.

Table 2. Asymmetry Factor (AF) Calculation

Sub-Watershed	Ar (Km <sup>2</sup> )	At (Km <sup>2</sup> )	AF	Tc*
1	1.42	2.55	55.69	3
2	0.71	1.50	47.33	3
3	2.33	3.44	67.73	1
4	1.52	3.56	42.70	2
5	0.66	1.04	63.46	2
6	0.19	0.66	28.79	1
7	0.28	0.44	63.64	2
8	0.84	1.88	44.68	3
9	1.64	2.42	67.77	1
10	0.44	1.37	32.12	1
11	0.36	0.59	61.02	2
12	0.39	0.67	58.21	2
13	0.5	1.27	39.37	2
14	0.36	1.45	24.83	1
15	0.42	0.64	65.63	1
16	0.31	0.52	59.62	2
17	1.97	3.4	57.94	2
18	0.4	1.49	26.85	1
19	0.44	1.00	44.00	3
20	2.16	3.32	65.06	1
21	0.28	0.97	28.87	1
22	0.91	1.68	54.17	3
23	1.04	2.89	35.99	2
24	0.73	1.53	47.71	3
25	0.61	1.35	45.19	3
26	0.26	0.65	40.00	2
27	0.78	1.51	51.66	3
28	0.89	2.06	43.20	3
29	2.01	4.47	44.97	3
30	2.15	3.92	54.85	3
31	1.44	2.76	52.17	3
32	0.55	1.02	53.92	3
33	0.28	0.97	28.87	1

\*Tc: Tectonic Class

### 3.2 The f Basin Shape Index (Bs)

Bs values in the study area calculated at 33 Sub-watersheds. Based on the calculation, the Bs value of the study area ranged from 0.97 (Sub-watershed 14) to 3.81 (Sub-watershed 4) (Tabel 3).

Table 3. Basin Shape Index (BS) Calculation

Sub-Watershed	Bl (m)	Bw (m)	Bs	Tc*
1	2998	1113	2.69	3
2	2179	935	2.33	3
3	3418	1358	2.52	3
4	4266	1121	3.81	2
5	1178	1040	1.13	3
6	1278	741	1.72	3
7	1344	463	2.90	3
8	2029	1332	1.52	3
9	2732	1506	1.81	3
10	2012	944	2.13	3
11	1469	536	2.74	3
12	1438	638	2.25	3
13	1568	1188	1.32	3
14	1430	1470	0.97	3
15	1481	660	2.24	3
16	1003	714	1.40	3
17	3414	1461	2.34	3
18	1903	1235	1.54	3
19	1839	883	2.08	3
20	2742	1623	1.69	3
21	2005	744	2.69	3
22	2305	1126	2.05	3
23	2686	1694	1.59	3
24	1944	1225	1.59	3
25	2078	1055	1.97	3
26	1513	554	2.73	3
27	2132	1212	1.76	3
28	3144	1044	3.01	2
29	4602	1370	3.36	2
30	4247	1416	3.00	2
31	2569	1160	2.21	3
32	1836	890	2.06	3
33	1849	702	2.63	3

\*Tc: Tectonic Class

In Figure 4, Bs class 2 seen in Sub-watershed 4, 28, 29, and 30, with the presence of fault structures around Sub-watershed 4. While the other 29 Sub-watershed classified as class 3, which are spread almost evenly across the study area, in several sub-watershed classes three, there are structures, namely fault, an anticline. Bs class 3 is estimated to be related to the tectonic process, which slows down or stops so that the shape of the watershed increasingly rounded. In general, based on Bs analysis, both sub-watershed based on sedimentary rocks and volcanic rocks, most of the Bs values are classified into tectonic class 3. This Bs value shows that the tectonic process is slowing down and the erosion process tends to develop more, causing the

shape of the watershed to become more rounded, the presence of *Bs* Class 2 is suspected as a result of the existence of structures in the sub-watershed.

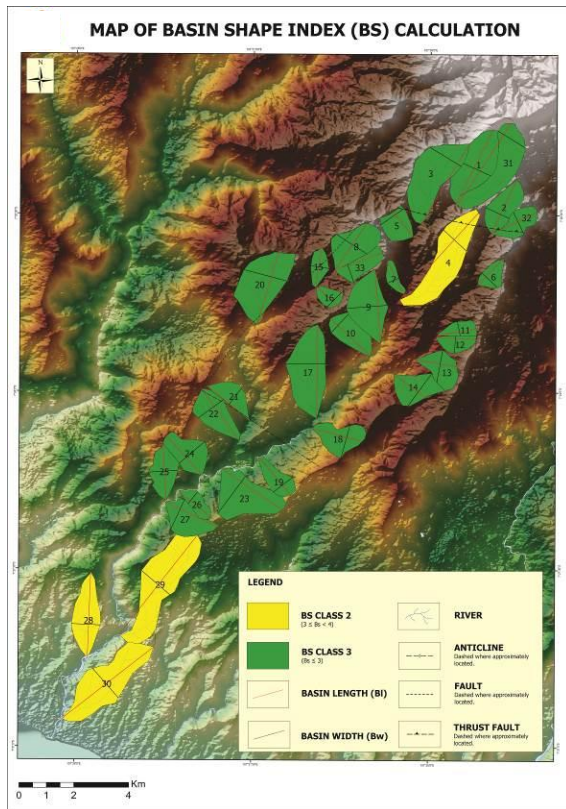


Fig 4: Map of Basin Shape Index (*Bs*) Calculation in Cilayu Watershed.

### 3.3 The Valley Floor Width-Valley Height Ratio (*Vf*)

The values of *Vf* for the study area shown in Table 4. Values of *Vf* vary from a low of 0.17 (Number 15) to a high of 2.04 (Number 23). According to [20], V-shaped valleys with low *Vf* values  $< 1$  develop in response to active uplift, and that broad U-shaped valleys with high *Vf* values  $> 1$  indicate significant lateral erosion, due to the stability of base level or to tectonic quiescence.

There are 15 *Vf* values which are classified into tectonic class 1 (High): 1(0.47), 6(0.43), 8(0.32), 9(0.32), 11(0.35), 12(0.38), 13(0.30), 14(0.37), 15(0.17), 18(0.36), 19(0.36), 21(0.37), 27(0.43), 30(0.49) and 33(28.87). 11 *Vf* values are classified into tectonic classes 2 (Moderate) and the other 7 *Vf* values which are classified into tectonic classes 3 (Low) (Table 4).

Table 4. Valley Floor Width-Valley Height Ratio (*Vf*) Calculation

No	<i>Vfw</i> (m)	<i>Eld</i> (m)	<i>Erd</i> (m)	<i>Esc</i> (m)	<i>Vf</i>	<i>Tc</i> *
1	13.85	83.03	31.59	28	0.47	1
2	53.92	109.51	87.75	51.87	1.15	3
3	32.71	220	188.52	151.52	0.62	2
4	40.03	96.93	88.06	13.68	0.51	2
5	189.43	225	192.83	76	1.43	3
6	32.02	244.97	210.47	153.14	0.43	1
7	100.92	317.52	249.01	156.41	0.80	2
8	32.62	401.68	425.03	310.68	0.32	1
9	31.29	455.72	442.2	352.25	0.32	1
10	171.48	510.22	473.39	388.97	1.67	3
11	30.11	554.82	542.74	462.85	0.35	1
12	34.99	574.89	536.41	463.7	0.38	1
13	28.5	651.45	638.42	550.09	0.30	1
14	26.34	763.63	731.08	677.11	0.37	1
15	20.98	900.13	906.84	779.27	0.17	1
16	48.59	1040.38	1116.23	987.26	0.53	2
17	56.44	1250.07	1232	1190.19	1.11	3
18	42.35	1437.63	1438.59	1320.85	0.36	1
19	47.18	1114.98	995.12	923.54	0.36	1
20	38.24	1184.89	1193.86	1138.83	0.76	2
21	42.15	1409.17	1354.58	1266.93	0.37	1
22	54.41	214.39	206.39	117.83	0.59	2
23	76.78	272.91	305.75	251.64	2.04	3
24	20.79	327.27	307.45	294.38	0.90	2
25	23.79	505.2	458.77	452.76	0.81	2
26	20.69	545.07	527.58	518.73	1.18	3
27	24.67	441.56	438.22	382.54	0.43	1
28	89.64	427.02	514.69	343.89	0.71	2
29	13.43	582.07	588.97	575.97	1.41	3
30	35.15	458.66	502.38	408.18	0.49	1
31	34.04	664.302	673.32	630.11	0.88	2
32	41.26	767.73	815.85	732.9	0.70	2
33	25.2	446.48	508.2	417.44	0.42	1

\**Tc*: Tectonic Class

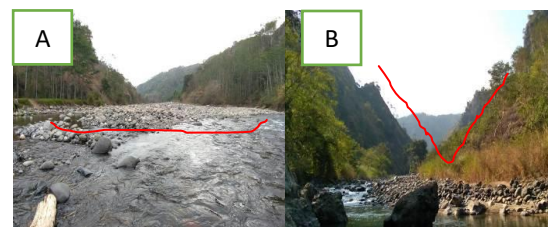


Fig 5: (A) U-shaped valley in the downstream area of the Cilayu watershed (B) V-shaped valley in the upper Cilayu watershed.

### 3.4 The Mountain-front Sinuosity Index (*Smf*)

The values of *Smf* for the study area shown in Table 5. Based on the results of calculations on 17

mountain-fronts, the *Smf* value in the study area varies-form low of 1.16 to a high of 2.54.

Based on the [22] classification, 10 *Smf* values included in class 1 (active tectonic class), and 7 *Smf* values included in class 2 (medium to weak tectonic classes). The index of active tectonics (IAT) values obtained after the *Smf* values are grouped based on the classification from [13]. 8 *Smf* values included in class 2 (moderate) and 9 *Smf* values included in class 3 (low) (Table 5).

**Table 5. Mountain-front Sinuosity Index (*Smf*) Calculation**

No.	<i>Lmf</i> (Km)	<i>Ls</i> (Km)	<i>Smf</i>	<i>Tc</i> *
1	3.29	2.61	1.26	2
2	1.63	1.41	1.16	2
3	2.76	2.02	1.37	2
4	7.25	3.51	2.07	3
5	3.76	2.15	1.75	3
6	2.54	1.73	1.47	2
7	2.01	1.53	1.31	2
8	2.15	1.40	1.54	3
9	1.76	1.39	1.27	2
10	2.25	1.85	1.22	2
11	5.33	2.57	2.07	3
12	2.98	1.47	2.03	3
13	3.94	2.17	1.82	3
14	3.02	1.47	2.05	3
15	2.16	1.69	1.28	2
16	3.28	1.29	2.54	3
17	1.59	0.85	1.87	3

\**Tc*: Tectonic Class

### 3.5 The Hypsometry Integral (*Hi*)

The hypsometry curve [19] is a comparison between the difference in relative height and relative area of a watershed. The total area (*A*) is the total horizontal surface area of the watershed. In comparison, the area value (*a*) is the surface area of a watershed bounded by a datum contour (specific elevation *h*).

*H* is the significant difference between the highest and lowest points of the watershed. The value of relative area (*a/A*) is always one at the lowest point of the watershed and the relatively high value (*h/H*) = 0. Moreover, the value of *a/A* is always 0 at the value of *h/H* = 1.

The hypsometry calculation reflects its lithology resistance influences the erosion status of an area. So it can also be used to identify lithology differences in a watershed.

*Hi*, values in the study area calculated at 33 Sub-watersheds. Based on the calculation, the *Hi* value of the study area ranged from 0.31 (Sub-watershed 12) to 0.61 (Sub-watershed 3) (Table 6).

**Table 6. Hypsometry Integral (*Hi*) Calculation**

Sub-Watershed	Hypsometry Integral ( <i>Hi</i> )	Tectonic Class
1	0.41	2
2	0.56	1
3	0.61	1
4	0.58	1
5	0.33	3
6	0.48	2
7	0.50	1
8	0.53	1
9	0.51	1
10	0.49	2
11	0.42	2
12	0.31	3
13	0.37	3
14	0.40	2
15	0.52	1
16	0.56	1
17	0.34	3
18	0.46	2
19	0.49	2
20	0.45	2
21	0.58	1
22	0.51	1
23	0.49	2
24	0.43	2
25	0.36	3
26	0.42	2
27	0.56	1
28	0.42	2
29	0.56	1
30	0.50	1
31	0.32	3
32	0.45	2
33	0.51	1

From the Hypsometry Integral (*Hi*) values in table 6, 7 sub-watersheds have *Hi* values > 0.55. The range of values, according to [19], is interpreted as youthful (convexity upward curves) where at this stage, an area has begun to experience an erosion process although it is not intensive. Characteristics of areas with youthful stages include the height of the maximum area having a large enough area and having a small area of difference in the area with a lower height.

A total of 10 sub-watersheds have a value of  $0.45 \geq Hi > 0.35$ , classified as the mature stage, where this stage occurs a balanced process between the erosion process and the process of removal, denudation, and other tectonic activities. The other 16 sub-watersheds have *Hi* value, which indicates the process of sub-watershed transition from the young to the middle stage and from the middle to the old stage.

According to [13], *Hi* values in the study area grouped into three classes, namely: Class 1 with a convex hypsometric curve ( $Hi \geq 0.5$ ), Class 2 with

a concave-convex curve ( $0.4 \leq H_i < 0.5$ ), and Class 3 with concave hypsometric curves ( $H_i < 0.4$ ).

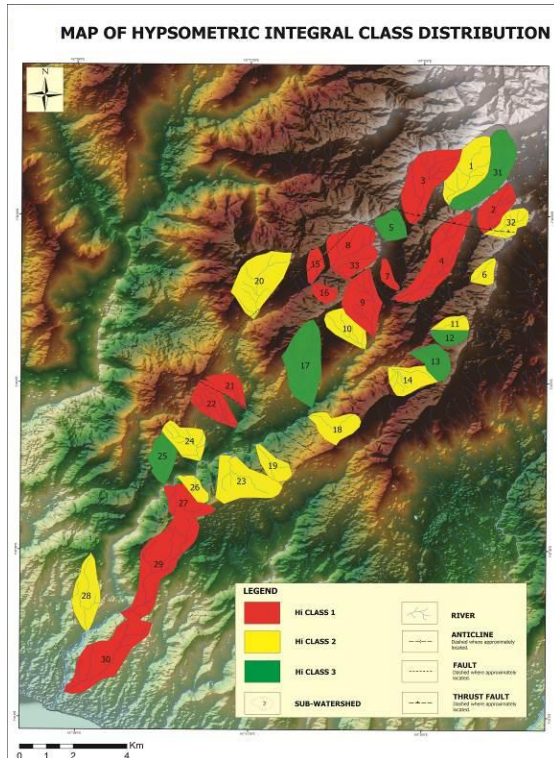
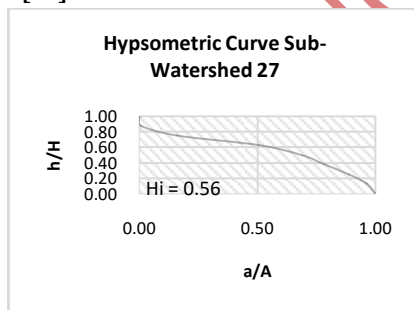


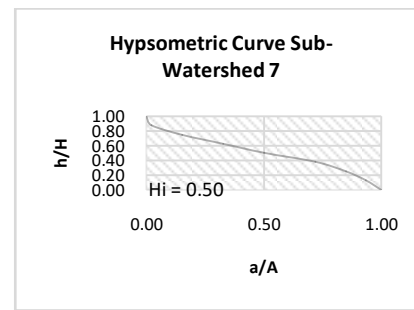
**Fig 6:** Map that shows the distribution of Hypsometric Integral Values based on classification of [13].

### 3.6 The Index of Active Tectonics (IAT)

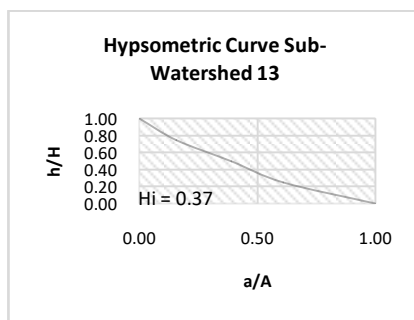
According to [13], *IAT* is obtained by the average of the different classes of geomorphic indices ( $S/n$ ) and divided into four classes, where class 1 is a very high tectonic activity with values of  $S/n$  between 1 and 1.5; class 2 is a high tectonic activity with values of  $S/n > 1.5$ , but  $< 2$ ; class 3 is moderately active tectonics with  $S/n > 2$  but  $< 2.5$ , and class 4 is low active tectonics with values of  $S/n > 2.5$ . *IAT* values in the research area are divided into four classes: Class 1 (very high), Class 2 (high), Class 3 (moderate), and Class 4 (low). *IAT* distributions in 33 sub-watersheds covering 119.97 km<sup>2</sup> are Class 1 around 1.78% of the watershed area (2.13 Km<sup>2</sup>), Class 2 around 7.03% of the watershed area (8.43 Km<sup>2</sup>), Class 3 around 30.61% of the watershed area (36,81 Km<sup>2</sup>), and Class 4 around 9.69% of the watershed area (11.62 Km<sup>2</sup>) (Table 7) (Figure 8). It explains that Cilayu Watershed dominantly has moderate to high tectonic activities.



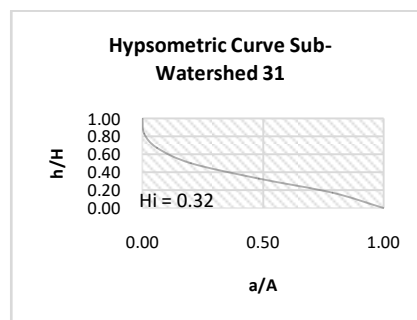
[A]



[B]



[C]



[D]

**Fig 7: Representative Hypsometric Curve from selected watershed which shown different stage [A] Youthful (Inequilibrium) stage [B] Transition stage from Youthful (Inequilibrium) to Mature (Equilibrium) stage [C] Mature (Equilibrium) Stage and [D] Transition stage from Mature (Equilibrium) to Monadnock Phase.**

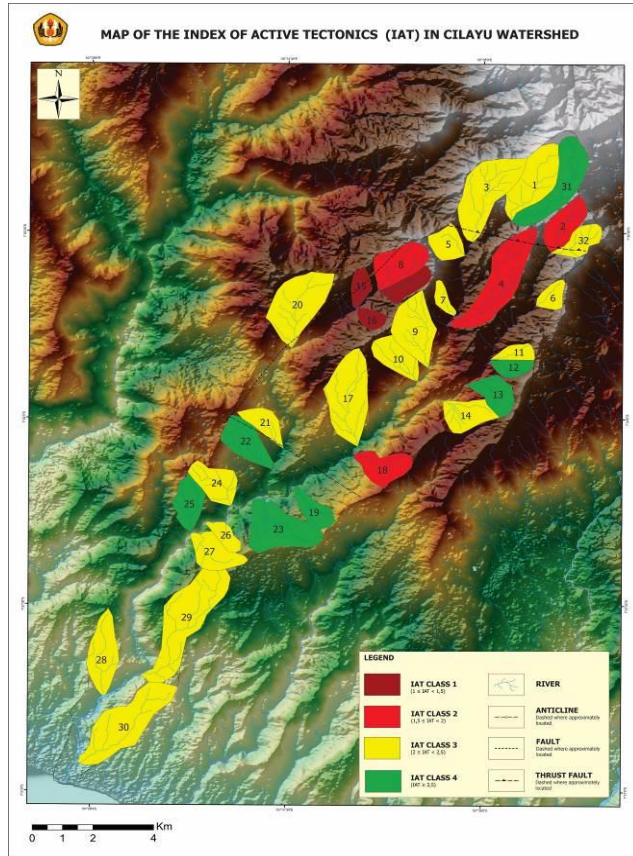


**Fig 8: Map that shows the distribution of Index of Active Tectonics (IAT) Values in Cilayu Watershed based on classification of [13].**

**Table 6. The Index of Active Tectonics (IAT) Calculation**

Sub-Watershed	AF	Bs	Vf	Smf	Hi	S/n	IAT
1	3	3	1	3	2	2.4	3
2	3	3	2	0	1	1.8	2
3	1	3	2	3	1	2.0	3
4	2	2	1	3	1	1.8	2
5	2	3	1	3	3	2.4	3
6	1	3	2	2	2	2.0	3
7	2	3	2	3	1	2.2	3
8	3	3	2	0	1	1.8	2
9	1	3	2	3	1	2.0	3
10	1	3	1	3	2	2.0	3
11	2	3	2	3	2	2.4	3
12	2	3	2	3	3	2.6	4
13	2	3	2	3	3	2.6	4
14	1	3	2	3	2	2.2	3
15	1	3	2	0	1	1.4	1
16	2	3	1	0	1	1.4	1
17	2	3	1	2	3	2.2	3

18	1	3	1	2	2	1.8	2
19	3	3	3	3	2	2.8	4
20	1	3	1	3	2	2.0	3
21	1	3	3	3	1	2.2	3
22	3	3	3	3	1	2.6	4
23	2	3	3	3	2	2.6	4
24	3	3	2	0	2	2.0	3
25	3	3	2	2	3	2.6	4
26	2	3	1	3	2	2.2	3
27	3	3	2	3	1	2.4	3
28	3	2	2	2	2	2.2	3
29	3	2	3	2	1	2.2	3
30	3	2	2	2	1	2.0	3
31	3	3	2	3	3	2.8	4
32	3	3	2	2	2	2.4	3
33	1	3	2	0	1	1.4	1

### 3.7 The Result of Field Observation

According to [21], the lineament associated with the geological structure could provide information about the tectonic activities. Field observation related to the evidence of the structure through landscape features shown in Fig. 9.

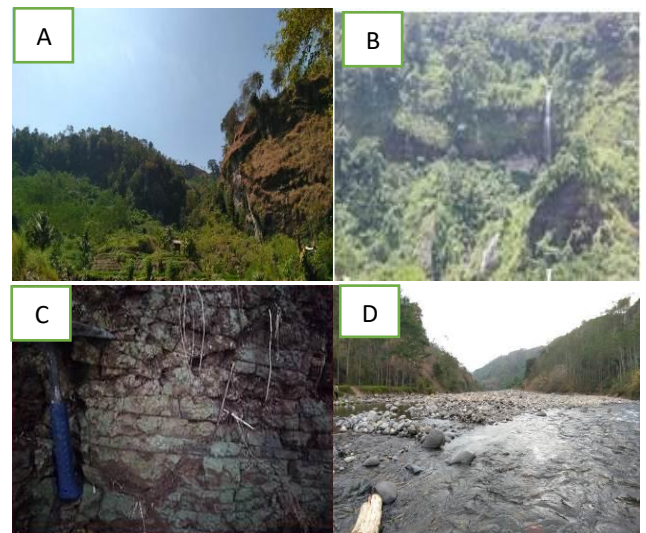


**Fig 9: (A) Morphology of Fault Scarp (B) Waterfall (C) Fracture zone (D) Depression zone occupied by alluvial deposits in the southern part of Cilayu watershed.**

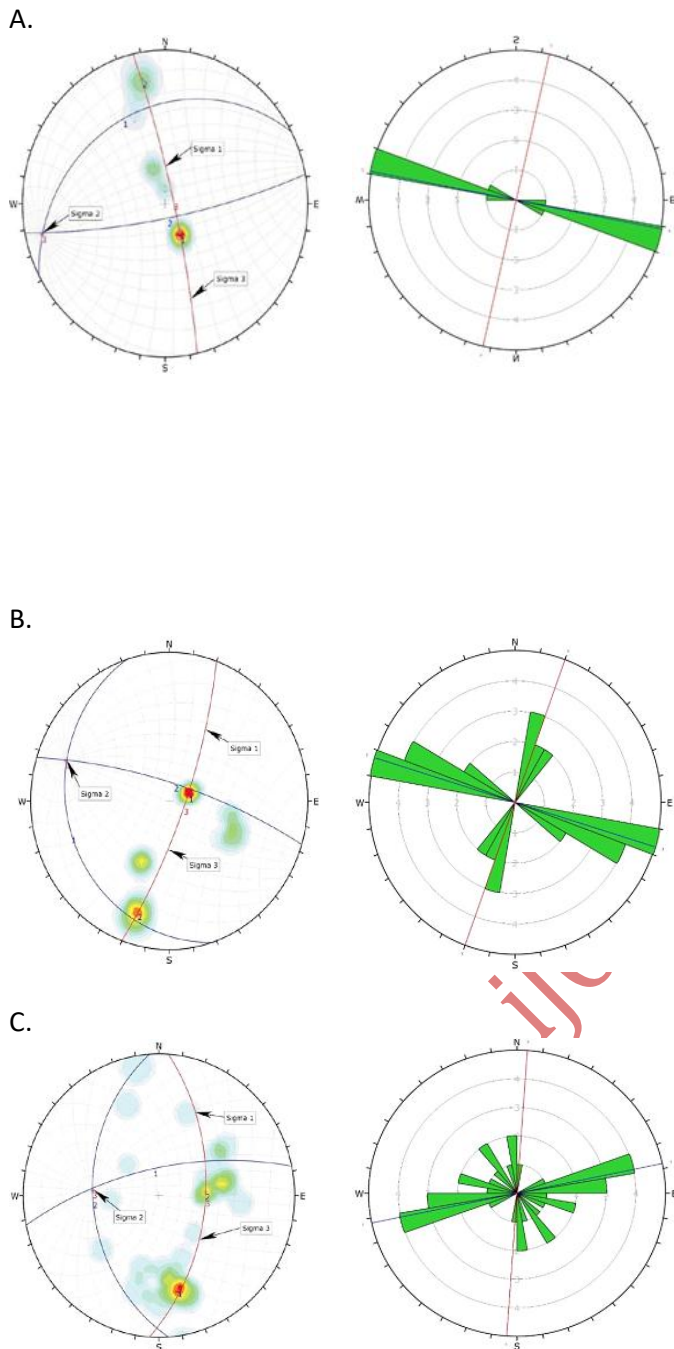


**Fig 10: Rosette and Stereonet Diagram from Joint Measurement Analysis (A) OP-17 in Cilayu River (B) OP-E, which located approximately in Rancadarandan and (C) OP-41 which located near Cikoneng.**

Joints measurements conducted in several locations of the fracture zone at Cilayu Watershed. Then the result of 'joint' measurement plotted into a rosette and stereonet diagrams. A summary of the site response analysis of the joint measurement shown in Fig. 10.

To simplify the reading of the joint measurement of each observation point result, we used the rosette and stereonet

diagrams. Rosette diagram informs about the fracture trend while the stereonet informs about the trend of the stress, which symbolizes with  $\sigma$ (sigma). In this location, the primary fracture trend relative to W-E and the dominant stress trend is N-S directions.

Stereonet diagram at OP-17 shows that the dominant stress is sigma 1 ( $\sigma_1$ ) with *Trend/Plunge* of N 0° E/62° indicating a normal fault. Stereonet diagram at OP-E shows that the dominant stress is sigma 3 ( $\sigma_3$ ) with *Trend/Plunge* of N 180° E/53° indicating a thrust fault. Furthermore, the stereonet diagram at OP-41 shows that the dominant stress is sigma 3 ( $\sigma_3$ ) with *Trend/Plunge* of N 138° /43° indicating a thrust fault.

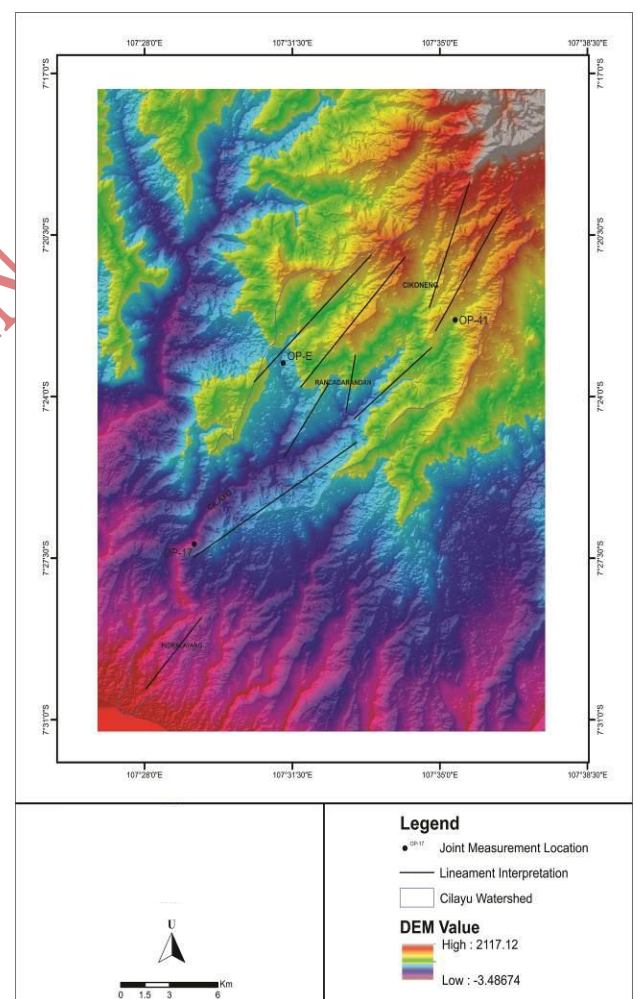


**Fig11: Lineament interpretation map of the study area related to the result of plotting joint on the rosette and stereo-net diagrams at OP-17, OP-41, and OP-E, which is shown in Fig. 9 before. They express that development of geological structure in Cilayu Watershed has main trends of faults; NE-SW directions.**

### 3.8 Discussion

The calculation result is indicating that the active-tectonic level took place at several parts of the study area. The values of *Af*, *Hi*, and *Vf* found to be high in the northern part of the area. The values of *Af* show widespread drainage basin asymmetry related to tectonic tilting. Active tectonic conditions in the study area also determined from the mountain-front sinuosity parameter index (*Smf*). Analysis of the variables *Smf* also supports a correlation between landscape and tectonic. *Smf* index values obtained from the calculation ranged from 1.16 to 2.54. This phenomenon shows that the case of uplift as an indication of tectonic activity in the watershed Cilayu. The values of *Vf* show that many valleys are narrow and deep, suggesting a high rate of incision associated with tectonic uplift. The Values of *Bs* show that the tectonic process is slowing down, and the erosion process tends to develop more, causing the shape of the watershed to become more rounded.

Therefore those analyses are confirmed by evidence found from fieldwork. The area which is affected by the active tectonic characterized by the presence of fractures in the rock, escarpment fault, ridge and valley lineaments. Morphotectonic characteristics in the Cilayu watershed can be an indication of the effect of active tectonics are as follows:

- The lineament of ridge and valley
- The lineament of drainage pattern
- The extreme curve of the river around Cibareg beg and Rancadarandan
- Broad depression zones and occupied by alluvial deposits in the southern part of Cilayu watershed.

Furthermore, the Joints at OP-17 show that the dominant tress is sigma 1 ( $s_1$ ) with *Trend/Plunge* of  $N 0^{\circ} E/62^{\circ}$  indicating a normal fault. The Joins at OP-E show that the dominant tress is sigma 3 ( $s_3$ ) with *Trend/Plunge* of  $N 180^{\circ} E/53^{\circ}$  indicating a thrust fault. Furthermore, Joints at OP-41 show that the dominant tress is sigma 3 ( $s_3$ ) with *Trend/Plunge* of  $N 138^{\circ} /43^{\circ}$  indicating a thrust fault.

It can conclude that Cilayu watershed has an active tectonic activity, which is confirmed by the result of field interpretation and quantitative geomorphic indices assessments. In order to validate the tectonic intensity, this study combines geomorphic indices to derive IAT value.

IAT values in the research area divided into four classes: Class 1 (very high), Class 2 (high), Class 3 (moderate), and Class 4 (low). IAT distributions in 33 sub-watersheds covering 119.97 km<sup>2</sup> are Class 1 around 1.78% of the watershed area (2.13 Km<sup>2</sup>), Class 2 around 7.03% of the watershed area (8.43 Km<sup>2</sup>), Class 3 around 30.61% of the watershed area (36,81 Km<sup>2</sup>), and Class 4 around 9.69% of the watershed area (11.62 Km<sup>2</sup>) (Table 7) (Figure 8). It

explains that Cilayu Watershed dominantly has moderate to high tectonic activities.

### 4. CONCLUSIONS

The Geomorphic indices computed using GIS considered to be suitable for evaluating the effects of active tectonics over Cilayu Watershed. To assess tectonic activity in the area, we analyzed fives geomorphic indices: the mountain front sinuosity index (*Smf*), valley floor width-to-height ratio (*Vf*), drainage basin asymmetry factor (*Af*), drainage basin shape (*Bs*), and hypsometric integral (*Hi*).

The values of *Af*, *Hi*, and *Vf* found to be high in the northern part of the area. The values of *Af* show widespread drainage basin asymmetry related to tectonic tilting while the values of *Smf* suggest that mountain fronts are tectonically active. The values of *Vf* show that many valleys are narrow and deep, suggesting a high rate of incision associated with tectonic uplift. The Values of *Bs* show that the tectonic process is slowing down, and the erosion process tends to develop more, causing the shape of the watershed to become more rounded.

About two-thirds of the Cilayu watershed has *Iat* values of classes 2 and 3, indicating moderately to highly active tectonics. Class 1 and 2 of *Iat*, indicative of the most active tectonics, occurs mainly in the northern part of the study area along the fault and fold zone. Class 3 of *Iat* corresponding to moderately active tectonics occurs over almost the whole study area, while Class 4 of *Iat* mainly takes place in the center of the study area.

The results confirm the usefulness of geomorphic indices analyses for assessing regional tectonics. They also suggest the necessity of future detailed research about tectonics in the study area. It expected the risk of disaster could minimize if, at any time, the disaster due to tectonic activity happens in the area.

### 5. ACKNOWLEDGMENTS

Our gratitude goes to the leaders of Universitas Padjadjaran for their support through the internal research grant of the 2020 RKDU scheme. Hopefully the results of this study will benefit the development of science and society.

### 6. REFERENCES

- [1] Molin, P., Pazzaglia, F.J., Dramis, F., "Geomorphic expression of active tectonics in a rapidly-deforming forearc, Sila Massif, Calabria, Southern Italy," *American Journal of Science* 304, 559–589, 2004.
- [2] Dumont, J.F., Santana, E., Vilema, W., "Morphologic evidence of active motion of the Zambapala Fault, Gulf of Guayaquil (Ecuador)," *Geomorphology* 65, 223–239, 2005.

- [3] Necea, D., Fielitz, W., Matenco, L., "Late Pliocene–Quaternary tectonics in the frontal part of the SE Carpathians: insights from tectonic geomorphology," *Tectonophysics* 410, 137–156, 2005.
- [4] Seeber, L., Gornitz, V., "River profiles along the Himalayan Arc as indicators of active tectonics," *Tectonophysics* 92, 335–367, 1983.
- [5] Brookfield, M.E., "The evolution of the great river systems of southern Asia during the Cenozoic India–Asia collision: rivers draining southwards," *Geomorphology* 22, 285–312, 1998.
- [6] Chen, Y.C., Sung, Q.C., Cheng, K.Y., "Along-strike variations of morphotectonic features in the Western Foothills of Taiwan: tectonic implications based on stream-gradient and hypsometric analysis," *Geomorphology* 56, 109–137, 2003.
- [7] Keller, E.A., Pinter, N., *Active Tectonics: Earthquakes, Uplift, and Landscape*. Prentice-Hall, New Jersey, 2002.
- [8] Kobor, J.S., Roering, J.J., "Systematic variation of bedrock channel gradients in the central Oregon Coast Range: implications for rock uplift and shallow landsliding," *Geomorphology* 62, 239–256, 2004.
- [9] E. Sukiyah, I. Syafri, A. Sjafrudin, E. Nurfadli, P. Khaerani, and D.A.P. Simanjuntak, "Morphotectonic and satellite imagery analysis for identifying quaternary fault at the southern part of Cianjur–Garut region, West Java, Indonesia," in *Proc. Asian Conference on Remote Sensing*, 2015, pp. 1–10.
- [10] Koesmono, K., Kusnama, & Suwarna, N., "Geological Map of Sindangbarang and Bandarwaru Sheet, Scale 1:100,000," 2nd edition, Geological survey Centre, Geology Agency, Bandung, 1996.
- [11] Alzwar M., Akbar N., & Bachri S., "Geological Map of Garut and Pameungpeuk sheet, Jawa, Scale 1: 100,000," 2nd edition, Geological survey Centre, Geology Agency, Bandung, 1992
- [12] Hare, P.W., Gardner, T.W., "Geomorphic indicators of vertical neotectonic along converging plate margins, Nicoya Peninsula, Costa Rica," In Morisawa, M., Hack, J.T. (Eds.), *Tectonic Geomorphology. Proceedings of the 15th Annual Binghamton Geomorphology Symposium*. Allen and Unwin, Boston, pp. 123–134, 1985.
- [13] El Hamdouni, R., Irigaray, C., Fernandez, T., Chacón, J., Keller, E.A., "Assessment of relative active tectonics, southwest border of Sierra Nevada (southern Spain)," *Geomorphology* 96, 150–173, 2007.
- [14] J.V. Pérez-Peña, A. Azor, J.M. Azañón, and E.A. Keller, "Active tectonics in the Sierra Nevada (Betic Cordillera, SE Spain): Insights from geomorphic indexes and drainage pattern analysis," *Geomorphology*, vol. 119, pp. 74–87, June 2010.
- [15] M. Dehbozorgi, M. Pourkermani, M. Arian, A.A. Matkan, H. Motamedi, and A. Hosseiniasl, "Quantitative analysis of the relative tectonic activity in the Sarvestan area, central Zagros, Iran," *Geomorphology* 121, 2010.
- [16] Bull, W.B., *Tectonic Geomorphology of Mountains: A New Approach to Paleoseismology*. Wiley-Blackwell, Oxford, 2007.
- [17] Ramírez-Herrera, M.T., "Geomorphic assessment of active tectonics in the Acambay Graben, Mexican volcanic belt," *Earth Surface Processes and Landforms* 23, 317–332, 1998.
- [18] Bull, W.B., McFadden, L., "Tectonic geomorphology north and south of the Garlock Fault, California. In: Doering, D.O. (Ed.), *Geomorphology in Arid Regions*," *State University of New York, Binghamton*, pp. 115–138, 1977.
- [19] Strahler, A.N., "Hypsometric (area–altitude) analysis of erosional topography," *Geological Society of America Bulletin* 63, 1117–1142, 1952.
- [20] Silva, P.G., Goy, J.L., Zazo, C., Bardaji, T., "Fault-generated mountain fronts in southeast Spain: geomorphologic assessment of tectonic and seismic activity," *Geomorphology* 50, 203–225, 2003.
- [21] E. Sukiyah, I. Syafri, B.J. Winarto, B. Susilo, A. Saputra, and E. Nurfadli, "Active faults and their implications for regional development in the southern part of West Java, Indonesia," in *Proc. The 24th annual scientific conference & exhibitions, Federation International Surveyors*, pp. 1–12, 2016.
- [22] Doornkamp, J. C. "Geomorphological Approaches to the Study of Neotectonics," *Journal of Geological Society*, Vol. 143: 335–342, 1986.